BULLETIN OF THE POLISH ACADEMY OF SCIENCES
TECHNICAL SCIENCES, Vol. 60, No. 1, 2012
DOI: 10.2478/v10175-012-0001-1

Transient stability analysis and control of power systems with considering flux decay by energy function approach

D. LU*, and X. ZHANG

School of Electronic, Information and Electrical Engineering, Shanghai Jiao Tong University, Shanghai 200240, China

Abstract. In this paper, transient stability of power systems with structure preserving models is considered. A Hamiltonian function which can be regarded as a Lyapunov function for the system is proposed. Based on this, the influence of flux decay dynamics, especially during a fault, on transient stability is analyzed. With the increase of load power, the variation of stability boundary in the rotor angle/E'_q plane is shown. The Energy-based excitation control, aiming at injecting additional damping into the post-fault system may reduce the critical clearing time (CCT). This can be demonstrated by the comparison of different flux decay dynamics in the fault-on condition, and the reason is illustrated by the relationship between rotor angle/E'_q and the stability boundary. An improved control strategy is proposed and applied to increase the CCT. Simulation results verify that improvement is obtained both in transient stability and dynamic performance.

Key words: transient stability, dynamic performance, flux decay, structure preserving models, energy function.

1. Introduction

With the increasing complexity of power systems, operating problems, such as transient instability and poor damping of oscillations, have been confronted. Generators and flexible AC transmission systems (FACTS) facilities play an important role in stability enhancement of power systems. However, the availability of FACTS is still limited, and their installation cannot be economically justified only on the basis of improving stability – a situation which will probably not be changed in a relatively brief time. Hence, excitation control remains the main input through which one can improve short-term (steady-state and transient) stability of power systems [1-3].

As the highly nonlinear nature of power systems, application of nonlinear control methods to enhance transient stability has attracted much attention. Some achievements using nonlinear control theories including the feedback linearization have been accomplished in the past [4, 5]. However, these control methods do not lend themselves easily to a physical interpretation of their action on the system. The problem may be solved by recent works on energy related design techniques [6–9]. The main advantage of these methods is that the physical structure is preserved and the closed-loop energy function can play the role of Lyapunov function. Though energy-based excitation control laws can dramatically improve the dynamic performance of power system, they may shorten the critical clearing time (CCT), which can be regarded as an important measure of transient stability margins.

The approach of energy function also makes the power system stability analysis more transparent, it is usually applied to assess the transient stability, estimate the CCT [10, 11] or provide a measure of system proximity to the point of maximum load ability [12, 13]. In this paper, a Hamiltonian function for the power system with a structure preserving model [14, 15] is presented to analyze the influence of flux decay dynamics on transient stability, which is not only related to the region of attraction about the operation point when flux decay circuits are considered. The reason why energy-based excitation controllers shorten the CCT is also presented. An improved control strategy to enhance the transient stability is proposed without decreasing the dynamic performance.

In order to establish a more realistic generator model, structure preserving models are chosen. These models are represented as a set of differential and algebraic equations (DAEs) and leave the structure of the network in its original form. The synchronous machine is modeled by the flux-decay E'_q model [15, 16] for the purpose of analysis.

2. Energy function of the structure preserving power system

A structure preserving power system with n machines, $n+m+1$ buses and voltage dependent loads is studied in this section. Buses from 1 to n are the terminal buses of the generators. Bus $n+1$ is an infinite bus. Buses from $n+2$ to $n+m+1$ are the load buses. For simplicity, it is assumed that the power network is lossless. The node admittance matrix is $\mathbf{Y} = [Y_{ij}] = [jB_{ij}]$, where B_{ij} is the susceptance of the line connecting bus i and j. The voltage of the i-th bus is expressed as $V_i \angle \theta_i$. All phase angles are measured relative to the infinite bus. The mechanical torque is assumed to be constant.

The i-th ($i = 1, \ldots, n$) machine is described as follows:

$$\dot{\delta}_i = \omega_i - \omega_0, \tag{1a}$$

$$\dot{\omega}_i = \frac{\omega_0}{M_i}\left(P_i^m - P_i^e\right) - \frac{D_i}{M_i}(\omega_i - \omega_0), \tag{1b}$$

*e-mail: doliyalu@msn.com

$$\dot{E'}_{qi} = \frac{x_{di} - x'_{di}}{T'_{d0i}} K_i + \frac{E_{fi}}{T'_{d0i}}. \tag{1c}$$

where

$$P_i^e = \frac{x'_{di} - x_{qi}}{2x_{qi}x'_{di}} V_i^2 \sin 2(\delta_i - \theta_i) + \frac{1}{x'_{di}} E'_{qi} V_i \sin(\delta_i - \theta_i),$$

$$K_i = -\frac{x_{di}}{x'_{di}(x_{di} - x'_{di})} E'_{qi} + \frac{1}{x'_{di}} V_i \cos(\delta_i - \theta_i),$$

δ_i is the rotor angle, ω_i is the rotor angle speed, $\omega_0 = 2\pi f_0$ is the synchronous machine speed, f_0 is the synchronous frequency, D_i is the damping constant, M_i is the inertia constant, x_{di}, x_{qi} are the direct and quadrature axis synchronous reactance respectively, x'_{di} is the direct axis transient reactance, E'_{qi} is the quadrature axis voltage behind transient reactance, P_i^m is the mechanical power, T'_{d0i} is the direct axis transient open-circuit time constant.

The real and reactive power demand at the i-th load bus are P_i^d and Q_i^d. The real power is represented as a constant, while the reactive power is depended on the voltage of the bus, i.e. $Q_i^d = Q_i^d(V_i)$. At the i-th ($i = 1, \ldots, n$) generator terminal bus, $P_i^d = Q_i^d = 0$, we get:

$$\begin{aligned} 0 = h_{1i} = &-\frac{x'_{di} - x_{qi}}{2x'_{di}x_{qi}} V_i^2 \sin 2(\delta_i - \theta_i) \\ &-\frac{E'_{qi}}{x'_{di}} V_i \sin(\delta_i - \theta_i) + \sum_{j=1}^{n+m+1} V_i V_j B_{ij} \sin\theta_{ij}, \end{aligned} \tag{1d}$$

$$\begin{aligned} 0 = h_{2i} = V_i^{-1} \Bigg(&\frac{x'_{di} + x_{qi}}{2x'_{di}x_{qi}} V_i^2 + \frac{E'_{qi}}{x'_{di}} V_i \cos(\delta_i - \theta_i) \\ &+\frac{x'_{di} - x_{qi}}{2x'_{di}x_{qi}} V_i^2 \cos 2(\delta_i - \theta_i) - \sum_{j=1}^{n+m+1} V_i V_j B_{ij} \cos\theta_{ij} \Bigg), \end{aligned} \tag{1e}$$

where h_{1i}, h_{2i} are the normal power flow equations.

At the i-th ($i = n+2, \ldots, n+m+1$) load terminal bus, we get:

$$0 = h_{1i} = \sum_{j=1}^{n+m+1} V_i V_j B_{ij} \sin\theta_{ij} - P_i^d, \tag{1f}$$

$$0 = h_{2i} = V_i^{-1} \left(- \sum_{j=1}^{n+m+1} V_i V_j B_{ij} \cos\theta_{ij} - Q_i^d \right). \tag{1g}$$

In general, the system (1) under research can be mathematically described in following affine nonlinear differential and algebraic system (NDAS):

$$\begin{cases} \dot{\boldsymbol{x}} = \boldsymbol{f}(\boldsymbol{x}, \boldsymbol{z}) + \boldsymbol{g}(\boldsymbol{x}, \boldsymbol{z})\boldsymbol{u} \\ 0 = \boldsymbol{h}(\boldsymbol{x}, \boldsymbol{z}) \end{cases}. \tag{2}$$

where

$$\boldsymbol{x} = (\boldsymbol{x}_1^T, \boldsymbol{x}_2^T, \ldots, \boldsymbol{x}_3^T)^T = (\boldsymbol{\delta}, \boldsymbol{\omega}, \mathbf{E'}_q)$$

is the state vector,

$$\boldsymbol{x}_i = (\delta_i, \omega_i, E'_{qi})^T, \qquad \boldsymbol{\delta} = (\delta_1, \delta_2, ..., \delta_n),$$
$$\boldsymbol{\omega} = (\omega_1, \omega_2, ..., \omega_n), \qquad \boldsymbol{E'}_q = (E'_{q1}, E'_{q2}, ..., E'_{qn}),$$

$$\boldsymbol{z} = (\boldsymbol{z}_1^T, \boldsymbol{z}_2^T, ..., \boldsymbol{z}_{n+m+1}^T)^T = (\boldsymbol{\theta}, \boldsymbol{V})$$

is the constraint vector,

$$\boldsymbol{z}_i = (\theta_i, V_i)^T, \qquad \boldsymbol{\theta} = (\theta_1, \theta_2, ..., \theta_{n+m+1}),$$
$$\boldsymbol{V} = (V_1, V_2, ..., V_{n+m+1}), \qquad \boldsymbol{u} = (u_1, u_2, ..., u_n)^T$$

is the input vector

$$u_i = E_{fi}/T'_{d0i}, \qquad \boldsymbol{f}(\boldsymbol{x}, \boldsymbol{z}) = (f_1, f_2, ..., f_n)^T,$$
$$\boldsymbol{f}_i(\boldsymbol{x}_i, \boldsymbol{z}_i) = (f_{i1}, f_{i2}, f_{i3})^T, \qquad f_{i1} = \omega_i - \omega_0,$$
$$f_{i2} = (\omega_0/M_i)(P_i^m - P_i^e) - (D_i/M_i)(\omega_i - \omega_0),$$
$$f_{i3} = -(x_{di}E'_{qi}/x'_{di}T'_{d0i}) + (x_{di} - x'_{di})V_i \cos(\delta_i - \theta_i)/x'_{di}T'_{d0i},$$
$$\boldsymbol{g}(\boldsymbol{x}, \boldsymbol{z}) = \mathrm{diag}\{\boldsymbol{g}_1, \boldsymbol{g}_2, ..., \boldsymbol{g}_n\}, \qquad \boldsymbol{g}_1 = (0, 0, 1)^T,$$
$$\boldsymbol{h}(\boldsymbol{x}, \boldsymbol{z}) = (\boldsymbol{h}_1, \boldsymbol{h}_2, ..., \boldsymbol{h}_n, \boldsymbol{h}_{n+2}, ..., , \boldsymbol{h}_{n+m+1})^T,$$
$$\boldsymbol{h}_i = (h_{1i}, h_{2i})^T.$$

The generator dynamics are described by differential equations while the bus voltage dynamics are described by algebraic load flow equations.

Consider the energy function given as follows:

$$H(\boldsymbol{x}, \boldsymbol{z}) = H_{KE} + H_{PE}, \tag{3a}$$

where

$$H_{KE} = \sum_{i=1}^{n} \frac{M_i}{2\omega_0} (\omega_i - \omega_0)^2, \tag{3b}$$

$$\begin{aligned} H_{PE} = &-\sum_{i=1}^{n} P_i^m (\delta_i - \delta_i^*) \\ &- \sum_{i=1, i\neq n+1}^{n+m+1} P_i^d (\theta_i - \theta_i^*) - \sum_{i=1, i\neq n+1}^{n+m+1} Q_i^d (\ln V_i - \ln V_i^*) \\ &- \sum_{i=1}^{n} \frac{(x'_{di} - x_{qi})}{4x'_{di}x_{qi}} \left(V_i^2 \cos 2(\delta_i - \theta_i) - V_i^{*2} \cos 2(\delta_i^* - \theta_i^*) \right) \\ &+ \sum_{i=1}^{n} \frac{x'_{di} + x_{qi}}{4x'_{di}x_{qi}} (V_i^2 - V_i^{*2}) + \sum_{i=1}^{n} \frac{x_{di}(E'^2_{qi} - E'^{*2}_{qi})}{2x'_{di}(x_{di} - x'_{di})} \\ &- \sum_{i=1}^{n} \frac{1}{x'_{di}} [E'_{qi} V_i \cos(\delta_i - \theta_i) - E'^*_{qi} V_i^* \cos(\delta_i^* - \theta_i^*)] \\ &- \sum_{i=1, i\neq n+1}^{n+m+1} \sum_{j=1}^{n+m+1} \left[V_i V_j B_{ij} \cos\theta_{ij} - V_i^* V_j^* B_{ij} \cos\theta_{ij}^* \right], \end{aligned} \tag{3c}$$

H_{KE} represents the kinetic energy, and H_{PE} represents the potential energy which can be expanded into several individual potential energy terms, is the stable equilibrium point (SEP). Indeed, function $H(\mathbf{x}, \boldsymbol{z})$ has an isolated local minimum at normal SEP. Hence it is a positive definite function in some neighborhood of SEP.

With the function $H(\boldsymbol{x}, \boldsymbol{z})$, NDAS (2) can be rewritten as follows:

$$\begin{cases} \dot{\mathbf{x}} = (\boldsymbol{J} - \boldsymbol{R})\partial_x H(\boldsymbol{x}, \boldsymbol{z}) + \boldsymbol{g}(\boldsymbol{x}, \boldsymbol{z})\mathbf{u} \\ 0 = \boldsymbol{h}(\boldsymbol{x}, \boldsymbol{z}) = \partial_z H(\boldsymbol{x}, \boldsymbol{z}) \end{cases}. \tag{4}$$

where

$$\partial_x H = (\partial_{x1} H, ..., \partial_{xn} H)^T,$$

$$\partial_{xi} H = (\partial_{\delta i} H, \partial_{\omega i} H, \partial_{E'qi} H)^T,$$

$$\partial_z H = (\partial_{z1} H, ..., \partial_{zn+m+1} H)^T,$$

$$\partial_{zi} H = (\partial_{\theta i} H, \partial_{Vi} H)^T,$$

$$\boldsymbol{J} = (\boldsymbol{J}_1, \boldsymbol{J}_2, ..., \boldsymbol{J}_n)^T,$$

$$\boldsymbol{J}_i = \begin{bmatrix} 0 & \omega_0/M_i & 0 \\ -\omega_0/M_i & 0 & 0 \\ 0 & 0 & 0 \end{bmatrix},$$

$$\boldsymbol{R} = (\boldsymbol{R}_1, \boldsymbol{R}_2, ..., \boldsymbol{R}_n)^T,$$

$$\boldsymbol{R}_i = \begin{bmatrix} 0 & 0 & 0 \\ 0 & \omega_0 D_i/M_i^2 & 0 \\ 0 & 0 & x_{di} - x'_{di}/T'_{d0i} \end{bmatrix}.$$

System (4) is actually a Hamiltonian realization [17, 18] of NDAS (2), and $H(x, z)$ acts as a Hamiltonian energy function.

3. Transient stability analysis based on the Hamiltonian function

3.1. Stability boundary with considering flux decay. Consider a single-machine-three-bus power transmission system showed in Fig. 1. The generator parameters are: $x_d = 0.162$, $x'_d = 0.047$, $x_q = 0.109$, $T'_{d0} = 6.8$ s, $M = 23.6$ s, $D = 5.0$.

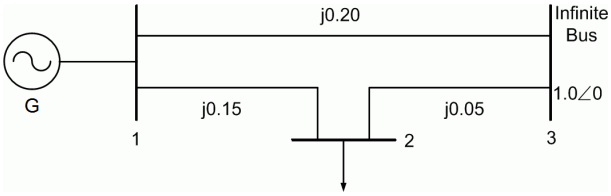

Fig. 1. A single-machine-three-bus power system

For simplification, it is assumed that $P^m = 3.5$ p.u., $Q_d = 0.5P_d$, and constant load power is considered. With the constant power load model, it is convenient to illustrate the influence of flux decay dynamics as the path of potential energy function H_{PE} is independent.

Definition 1. For the compact set C_k, $\det \boldsymbol{J}_l|_{(\boldsymbol{x},\boldsymbol{z})\in C_k} \neq 0$ and $\boldsymbol{J}_l|_{(\boldsymbol{x},\boldsymbol{z})\in C_k}$ has $k(k > 0)$ negative eigenvalues [19].

$\boldsymbol{J}_l$ is the Jacobian of the load flow equations and $\boldsymbol{J}_l = \partial \boldsymbol{h}/\partial \boldsymbol{z}$. The potential energy sheets under $P^d = 2.5$ p.u. are drawn in Fig. 2. It can be seen that the system has two potential energy sheets. The lower one belongs to C_0 while the upper one belongs to C_1.

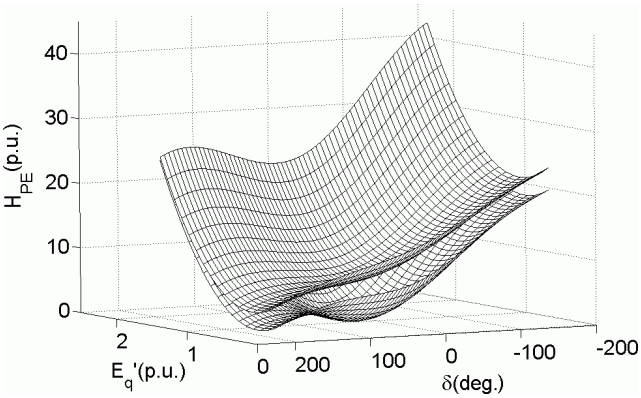

Fig. 2. Potential energy sheets under $P^d = 2.5$ p.u.

It could be judged from the potential energy surfaces in Fig. 2 that the upper one has no energy well. And the state of the system could not be kept on it. For the open-loop system, there are often several solutions to the equilibrium load flow equations. Usually only one of the power flow solutions corresponds to a practical SEP. This solution, which will be denoted as the "operable" solution, is angularly stable for the system in sheet C_0. The other solutions typically correspond to unstable equilibrium points (UEPs) of the power system, even though some of them in C_k are also angularly stable [20].

Put our focus on C_0. Figure 3 shows the contour lines of the potential energy sheet C_0 in δ/E'_q plane under $P^d = 2.5$ p.u. It can be seen that the potential energy function is positive definite about the operating point. The SEP defines a local minimum of the energy and occupies the bottom of the energy well. The UEP of which the energy is the minimum on the boundary represents the easiest path to escaping from SEP.

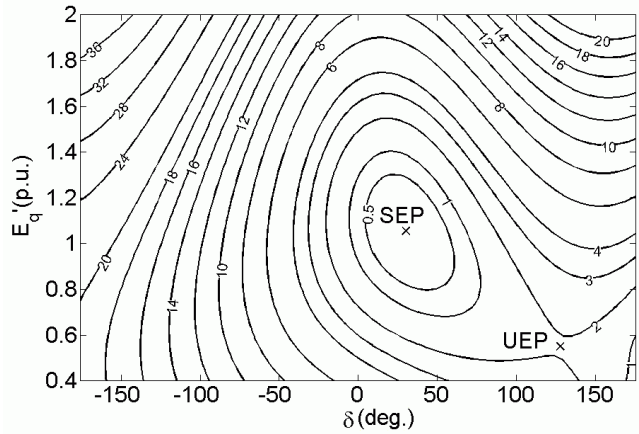

Fig. 3. Contour of potential energy surface under $P^d = 2.5$ p.u.

Figure 4 shows the contour lines of potential energy surface under heavy load of $P^d = 5.0$ p.u. The increase of load shrinks the energy well and lowers the potential energy of UEP. The impasse surface appears which is presented by the dashed line.

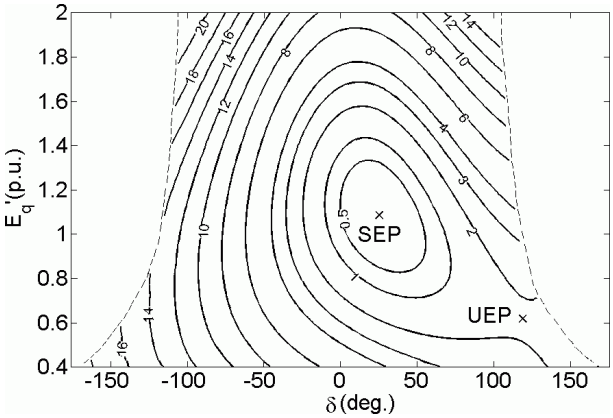

Fig. 4. Contour of Potential energy surface under $P^d = 5.0$ p.u.

If the state exits in the vicinity of UEP, the rotor angle will vary rapidly. The disturbance is clearly an angle instability phenomenon. For transient conditions, voltage collapse may occur as a bifurcation of the transient power flow equations. The implicit function theorem may be used to define the bus voltage variables $z = (\theta, V)$ as smooth functions of the generator rotor angles and E'_q in a neighborhood of a solution under $\det J_l|_{(\boldsymbol{x},\boldsymbol{z})\in C_k} \neq 0$. As the rotor angles and E'_q vary, the bus voltage variables also vary in a smooth fashion so as to satisfy the load flow equations. However, when the power flow fails to converge, the solution trajectory vanishes in the vicinity of the impasse surface (singular surface):

$$IS = \{(x, z)|h(x, z) = 0, \det(J_l) = 0\}. \tag{5}$$

If impasse surface is reached, the system behavior becomes unpredictable, (θ, V) are no longer dependent on (δ, E'_{qi}). The generators rotor angles and E'_q become the parameters for the bifurcation of the load flow equation. Singular perturbation methods can be applied [20]. The system will experience voltage collapse before angle instability.

If a heavier load is applied, there will be no UEP in C_0, and only Voltage collapse can occur due to the large disturbance.

Roughly speaking, at the same rotor angle the higher E'_q is, the longer distance to the boundary of potential energy well is. It means that at a higher value of E'_q the rotor angle may experience larger variation before the system trajectory jumps out of the energy well. So if we fix a high field voltage during a fault, the initial state of post-fault system may be far from the boundary of an energy well. And the total energy may be not sufficient to drive the trajectory out of the energy well because the boundary of potential energy well at a high E'_q is much higher than the one at a low value of E'_q. Therefore, the CCT increases. Hence, the larger field voltage during any admissible fault, the "more stable" system is. This is consistent with the simulation results in [21]. For a physical reason, since the mechanical power does not vary substantially in such a short time, the generators tend to accelerate driving the system state away from the operating point. It is possible to reduce this acceleration, and thus shorten the system trajectory in the fault-on condition, by somehow increasing the electrical power delivered.

3.2. Stability analysis with considering control effect. According to system (4), we have that $\partial H/\partial \boldsymbol{z} = \boldsymbol{h} = 0$. Then the time derivative of $H(\boldsymbol{x}, \boldsymbol{z})$ is:

$$\begin{aligned} \dot{H} = &-\sum_{i=1}^{n} \frac{D_i}{\omega_0}(\omega_i - \omega_0)^2 \\ &-\sum_{i=1}^{n} \frac{x_{di} - x'_{di}}{T'_{d0i}} K_i^2 - \sum_{i=1}^{n} K_i u_i. \end{aligned} \tag{6}$$

If $u_i = 0$, it is the open-loop case. The system damping can be enhanced by adding a negative definite term to the Lyapunov derivative. The control law can be expressed as:

$$u = [a_1 K_1, \ldots, a_n K_n]^T. \tag{7}$$

Actually, this control law is the extension of so-called LgV controller [22] in the structure preserving system.

Then we have:

$$\dot{H} = -\sum_{i=1}^{n} \frac{D_i}{\omega_0}(\omega_i - \omega_0)^2 - \sum_{i=1}^{n} \left(\frac{x_{di} - x'_{di}}{T'_{d0i}} + a_i \right) K_i^2. \tag{8}$$

Because the system is stable at the operating point, it can be seen from the dynamic system theory that the system converges to the largest invariant set contained in:

$$\begin{aligned} E &= \left\{ x, z : \dot{H}(x, z) = 0, h = 0 \right\} \\ &= \{ x, z : \omega_i = \omega_0, K_i = 0, h = 0 \}. \end{aligned} \tag{9}$$

From $\omega_i \equiv \omega_0$, we can get that $P_i^m - P_i^e = 0$, $i = 1, \ldots, n$.

Thus, the point in the largest invariant set satisfies:

$$\begin{cases} f(x, z) = 0 \\ h(x, z) = 0 \end{cases}, \tag{10}$$

which is exactly the condition the equilibrium point satisfies. Hence there exists a suitably small neighbor- hood Ω of the operating point such that the largest invariant set in Ω only contains one point, i.e., the operating point. From the LaSalle's invariance principle, the closed-loop system with the control law (7) ensures asymptotic stability of the desired SEP with the function $H(\boldsymbol{x}, \boldsymbol{z})$, which can be regarded as the Lyapunov function.

H_{PE} is the potential energy function both for open-loop system and closed-up system. It gives a way to compare the effect of control with the open-loop case under the same condition and find the reason why the CCT shortens.

The response of the system to a short-circuit at the machine's terminal will be studied. The pre-fault and post-fault systems are identical. The transient process is stimulated at $t = 1.0$ s and restored at $t = 1.1$ s, clearing time: $t_{cl} = 0.1$ s. Figure 5 shows the close-loop system trajectory superimposed on the potential energy surface from Fig. 3. The energy well is only valid for post-fault trajectory. The dashed curve represents the fault-on trajectory which is shown only to illustrate the state space trajectory during the fault, and the solid line represents the post-fault trajectory. Figure 6 shows the response of rotor angle. It can be seen from Fig. 5 and Fig. 6 that the excitation controller provides the system with good damping.

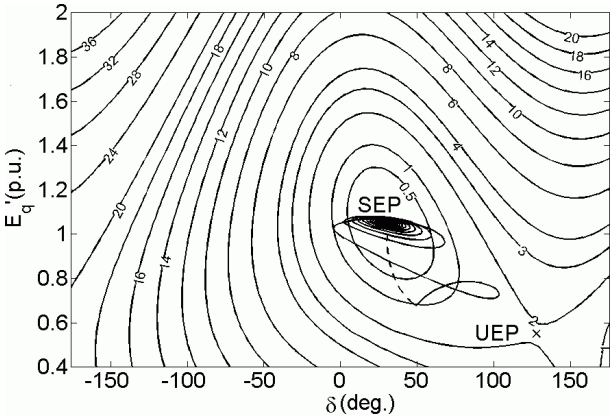

Fig. 5. Trajectory of the system with excitation control ($t_{cl} = 0.1$ s)

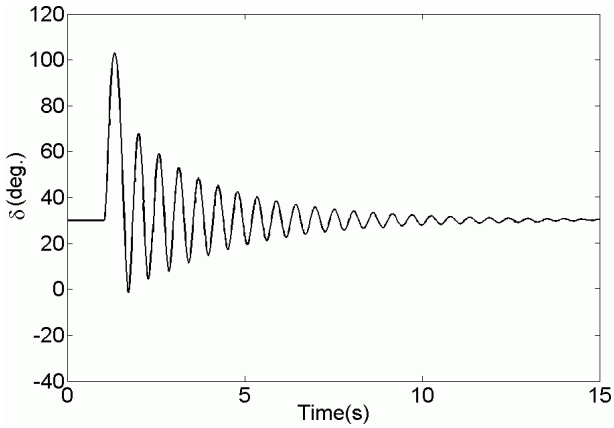

Fig. 6. Response of rotor angle with excitation control ($t_{cl} = 0.1$ s)

Figure 7 shows the closed-loop system trajectory when the fault clearing time is set to be 0.12 s. For the same conditions, Fig. 8 shows the trajectory of open-loop system, and Fig. 9 shows the response of rotor angle. It can be seen that the closed-loop system loses stability while the open- loop one keeps under $t_{cl} = 0.12$ s.

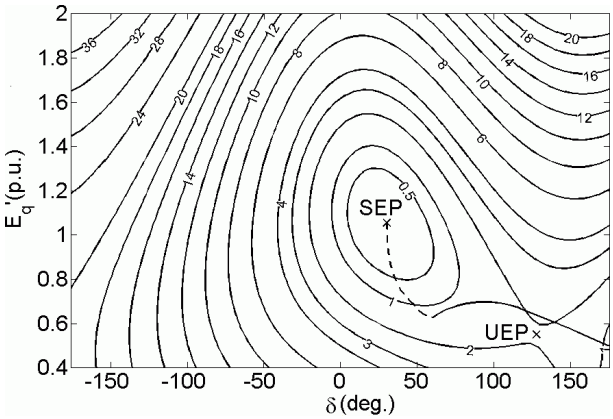

Fig. 7. Trajectory of the system with excitation control ($t_{cl} = 0.12$ s)

In Figs. 7 and 8, the voltages drop during fault, the same E'_q does. Especially in Fig. 7, E'_q drops dramatically. The total energy of the initial state in post-fault system is large enough to jump out of the energy well. In the classical power system model, the transient stability only relates to the region of attraction. With the flux decay circuit, the transient stability also relates to the flux decay dynamics. The CCT not only reflects the region size of stability but also the performance of the excitation control. Here, the decreased CCT may be considered as a result of the bad flux decay dynamics during the fault.

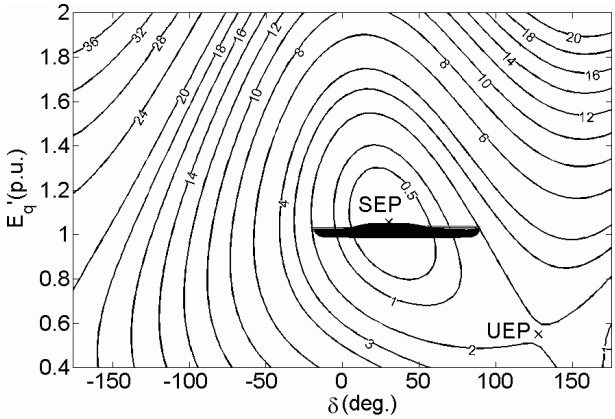

Fig. 8. Trajectory of the open-loop system ($t_{cl} = 0.12$ s)

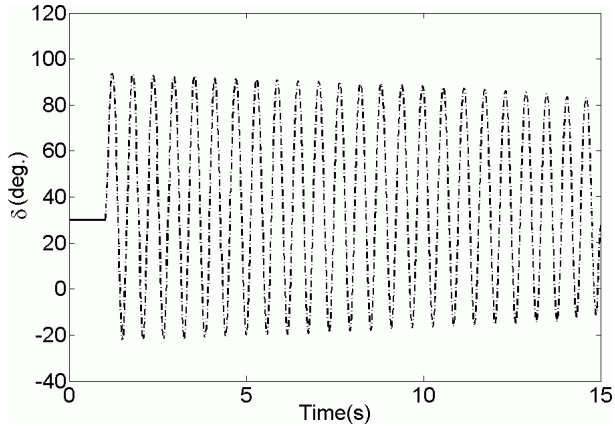

Fig. 9. Response of rotor angle with open-loop ($t_{cl} = 0.12$ s)

4. An improved excitation control strategy

According to the analysis in Subsec. 3.1, upgrading the field voltage during the fault has good effect on the improvement of CCT. The proposed control strategy is given as follows: during the severe fault, generators field voltage is set to the maximum available value (also called the 'ceiling voltage') instead of excitation controller (7); after the fault, the excitation controller is applied again to add damping and accelerate the convergence of the system.

Simulation results are presented in Figs. 10 and 11 to show the behavior of the closed-loop system with the proposed control method.

It can be seen that the CCT has been increased with the improved control strategy which still provides a good dynamic performance in damping the system oscillation. It offers an effective way to meet the conflicting exciter performance requirements with regard to system stability.

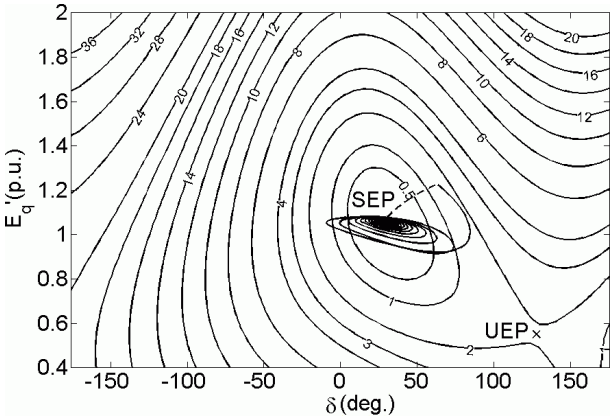

Fig. 10. Trajectory of the system with proposed control ($t_{cl} = 0.12$ s)

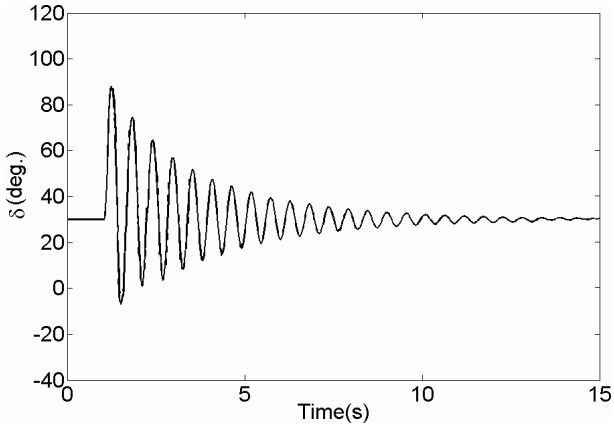

Fig. 11. Response of rotor angle with proposed control ($t_{cl} = 0.12$ s)

5. Conclusions

The transient stability of power system including flux decay is related to the domain of attraction and the flux decay dynamics. In this paper, the influence of flux circuit dynamics on transient stability of structure preserving power system is analyzed based on the approach of energy function. The relationship between the rotor angle/E'_q and the boundary of energy well is illustrated. According to the characteristics of the system, the variation of the stability boundary in rotor angle/E'_q plane with different loading conditions is shown. The extension of the design of the LgV excitation controller is presented. The reduction of system CCT with excitation controller is mainly caused by the decrease of E'_q during a fault, which makes the state of a system close to the UEP. An improved control method is proposed. The simulation results show the effectiveness of the proposed method in improving the transient stability and dynamic performance of power systems.

REFERENCES

[1] P. Kundur, *Power System Stability and Control*, McGraw-Hill, New York, 1994.

[2] N. Hingorani and L. Gyugyi, *Understanding FACTS: Concepts and Technology of Flexible AC Transmission Systems*, IEEE, New York, 2000.

[3] T. Kaczorek, "Improvement in the efficiency of the distributed power systems", *Bull. Pol. Ac.: Tech.* 57 (4), 369–374 (2009).

[4] Q. Lu, Y. Sun, Z. Xu, and T. Mochizuki, "Decentralized nonlinear optimal excitation control", *IEEE Trans. Power Syst.* 11 (4), 1957–1962 (1996).

[5] Q. Lu, Y. Sun, and S. Wei, *Nonlinear Control Systems and Power System Dynamics*, Kluwer Academic Publishers, Boston, 2001.

[6] S. Arimoto, "Passivity- based control", *Proc. IEEE ICRA'00 Conf.* 1, 227–232 (2000).

[7] A. Van Der Schaft, *L_2-gain and Passivity Techniques in Nonlinear Control*, Springer-Verlag Press, Berlin, 2000.

[8] Y. Wang, G. Feng, D. Cheng, and Y. Liu, "Adaptive L_2 disturbance attenuation control of multi-machine power systems with SMES units", *Automatica* 42 (7), 1121–1132 (2006).

[9] V. Azbe and R. Mihalic, "The control strategy for an IPFC based on the energy function", *IEEE Trans. Power Syst.* 22 (4), 1662–1669 (2008).

[10] Y. Zou, M. Yin, and H. Chiang, "Theoretical foundation of the controlling UEP method for direct transient-stability analysis of network-preserving power system models", *IEEE Trans. Circ. Syst. I: Fundam. Theory Appl.* 50 (10), 1324–1336 (2003).

[11] D. Fang and Y. Qin, "A new trajectory sensitivity approach for computations of critical parameters", *Electr. Power Syst. Res.* 77 (3–4), 303–307 (2007).

[12] R. Mihalic and U. Gabrijel, "Transient stability assessment of systems comprising phase-shifting FACTS devices by direct methods", *Int. J. Electr. Power and Energy Syst.* 26 (6), 445–453 (2004).

[13] A. Abdelaziz, M. Abu-Elnaga, and M. Elsharkawy, "Voltage stability assessment of multi-machine power systems using energy function and neural networks techniques", *Electr. Power Comp. and Syst.* 34 (12), 1313–1330 (2006).

[14] N. Tsolas, A. Arapostathis, and P. Varaiya, "Structure preserving energy function for power system transient stability analysis", *IEEE Trans. Circ. Syst.* 32 (10), 1041–1049 (1985).

[15] B. He, X. Zhang and X. Zhao, "Transient stabilization of structure preserving power systems with excitation control via energy-shaping", *Int. J. Electr. Power and Energy Syst.* 29 (10), 822–830 (2007).

[16] C. Chu and H. Chiang, "Constructing analytical energy functions for network-preserving power system models", *Circ. Syst. Signal Proc.* 24 (4), 363–383 (2005).

[17] R. Ortega, A. Van Der Schaft, and B. Maschke, "Interconnection and damping assignment passivity-based control of port-controlled Hamiltonian systems", *Automatica* 38 (4), 585–596 (2002).

[18] M. Galaz, R. Ortega, A. Bazanella, and A. Stankovic, "An energy-shaping approach to the design of excitation control of synchronous generators", *Automatica* 39 (1), 111–119 (2003).

[19] Y. Makarov, D. Hill, and I. Hiskens, "Properties of quadratic equations and their application to power system analysis", *Int. J. Electr. Power and Energy Syst.* 22 (5), 313–323 (2000).

[20] K.L. Praprost and K.A. Loparo, "An energy function method for determining voltage collapse during a power system transient", *IEEE Trans. Circ. Syst. I: Fundam. Theory Appl.* 41 (10), 635–651 (1994).

[21] Y. Sun, X. Li, M. Zhao, and Y. Song, "New Lyapunov function for transient stability analysis and control of power systems with excitation control", *Electr. Power Syst. Res.* 57 (2), 123–131 (2001).

[22] A. Bazanell and C. Conceicao, "Transient stability improvement through excitation control", *Int. J. Robust and Nonlinear Control* 14 (9–10), 891–910 (2004).